



Cite this: *Chem. Commun.*, 2015, 51, 2946

Received 5th December 2014,
Accepted 8th January 2015

DOI: 10.1039/c4cc09743b

www.rsc.org/chemcomm

Homolytic H₂ cleavage by a mercury-bridged Ni(II) pincer complex $\{[(\text{PNP})\text{Ni}]_2\{\mu\text{-Hg}\}\}^\dagger$

Markus Kreye,^a Matthias Freytag,^a Peter G. Jones,^a Paul G. Williard,^b
Wesley H. Bernskoetter^{*b} and Marc D. Walter^{*a}

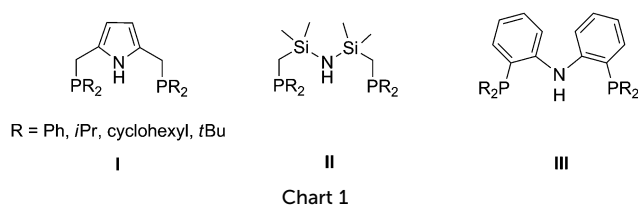
Reduction of the pincer nickel(II) complex $[(\text{PNP})\text{NiBr}]$ with sodium amalgam (Na/Hg) forms the mercury-bridged dimer $\{[(\text{PNP})\text{Ni}]_2\{\mu\text{-Hg}\}\}$, which homolytically cleaves dihydrogen to form $[(\text{PNP})\text{NiH}]$. Reversible CO₂ insertion into the Ni–H bond is observed for $[(\text{PNP})\text{NiH}]$, forming the monodentate $\kappa^1\text{O}$ -formate complex $[(\text{PNP})\text{NiOC(O)H}]$.

Pincer ligands have become a highly topical field of chemical research in recent years because of their readily modifiable steric and electronic properties. This, together with the high thermal stability of their metal complexes, makes them highly attractive ligands in small molecule activation and catalysis.¹ Combinations of pincer ligands and environmentally benign 3d-elements have been of particular interest in catalyst development for hydrofunctionalizations,² cross-coupling reactions,³ CH-bond⁴ or CO₂ activation⁵ and dehydrogenation reactions.⁶ In this context, nickel has shown promise for catalytic cross-coupling,^{3b,7} olefin hydrogenation⁸ and CO₂ reduction.⁵ These precedents were the motivation for our studies on sterically encumbered monoanionic pyrrolyl-based PNP pincer systems and their phosphine-substituted derivatives (**I**, Chart 1). The phenyl-substituted PNP ligand was introduced independently in 2012 by the groups of Tonzetich,⁹ Gade¹⁰ and Mani,¹¹

who employed this support in the synthesis of nickel and palladium complexes.

In comparison to the related amine- and diphenylaniline-derived PNP-ligands **II**¹² and **III**,¹³ the pyrrolyl-based system **I** has received less attention (Chart 1). In this contribution we report on the preparation and reactivity of the *t*Bu-(**1a**)^{3b} and *i*Pr-(**1b**)¹⁴ substituted PNP nickel pincer systems (ESI[†]). X-ray structures of **1b** and the lithium salt **2a** are reported in the ESI.[†] The *t*Bu-substituted derivative was employed to stabilize a remarkable Hg-bridged dinickel species exhibiting an interesting electronic structure, which enables this complex to act as a source of the (PNP)Ni fragment. This was illustrated by the homolytic cleavage of H₂ to give (PNP)NiH. The insertion chemistry of CO₂ into the Ni–H bond is also briefly discussed.

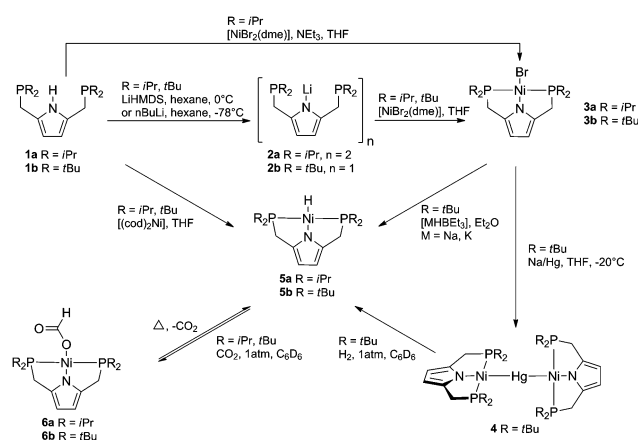
The nickel(II) bromide species $[(^R\text{PNP})\text{NiBr}]$ (**3**) may be synthesised in moderate yields (40–52%) starting either from **1a** and $[\text{NiBr}_2(\text{dme})]$ (dme = 1,2-dimethoxyethane) in the presence of NEt₃ or the isolated lithium salts $[(^R\text{PNP})\text{Li}]_n$ (**R** = *i*Pr, *n* = 2, **2a**; **R** = *t*Bu, **2b**) and $[\text{NiBr}_2(\text{dme})]$ (Scheme 1). The lithium salts are best prepared from the reaction of **1** with $\text{Li}[\text{N}(\text{SiMe}_3)_2]$ in hexane at 0 °C or by addition of *n*BuLi to a hexane solution of **1** at –78 °C (ESI[†]).



^a Institut für Anorganische und Analytische Chemie, Technische Universität, Braunschweig, Hagenring 30, 38106 Braunschweig, Germany.
E-mail: mwalter@tu-bs.de

^b Department of Chemistry, Brown University, Providence, RI 02912, USA.
E-mail: wb36@brown.edu

[†] Electronic supplementary information (ESI) available. CCDC 1037224–1037231. For ESI and crystallographic data in CIF or other electronic format see DOI: 10.1039/c4cc09743b



Scheme 1



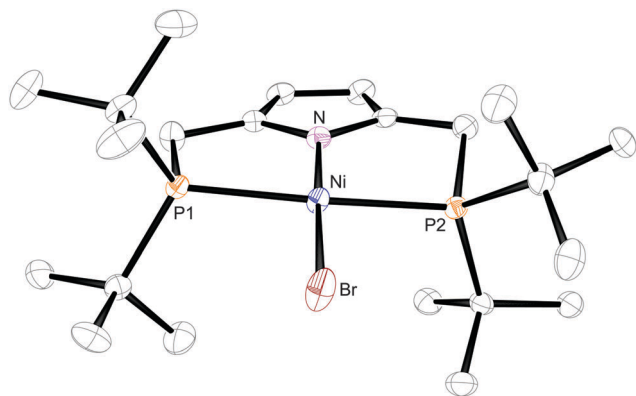


Fig. 1 Displacement ellipsoid plot (50% probability) of $[(t\text{BuPNP})\text{NiBr}]$ (**3b**). Hydrogen atoms are omitted for clarity. Selected bond distances (Å) and angles ($^\circ$): Ni–N 1.8520(18), Ni–P1 2.2407(6), Ni–P2 2.2270(6), Ni–Br 2.3175(4), N–Ni–Br 178.67, P1–Ni–P2 167.90(2), N–Ni–P1 84.51(6), N–Ni–P2 84.32(6), P1–Ni–Br 96.778(19), P2–Ni–Br 94.371(19).

The molecular structure of **3b** (Fig. 1) features the expected square planar geometry at the nickel atom with an Ni–N distance of 1.8520(18) Å and N–Ni–Br angle of 178.67(6) $^\circ$.

Previous electrochemical studies indicate that $[(\text{PhPNP})\text{NiCl}]$, $[(\text{CyPNP})\text{NiCl}]$ and $[(t\text{BuPNP})\text{NiCl}]$ can be reduced below *ca.* -2 V (vs. Fc/Fc^+) in THF.^{3b} However, $[(\text{PhPNP})\text{Ni}]_2^{10}$ is the only example in which the identity of the PNP–Ni(i) species is definitively established.³ Monomeric Ni(i) complexes are radicals and therefore highly reactive species, which makes their isolation challenging. Nevertheless, Ni(i) complexes have been proposed as catalytically competent species in C–S cross-coupling.^{3b} Despite the dearth of other examples, we attempted to isolate such a Ni(i) complex of **3b** using commonly employed reducing reagents such as KC_8 and Na/Hg . Although no isolable product was obtained with KC_8 , reduction with Na/Hg in THF gives an intense dark red solution, from which the diamagnetic, mercury-bridged dimer $[(t\text{BuPNP})\text{Ni}]_2(\mu\text{-Hg})$ (**4**) is isolated (Scheme 1, ESI †). Complex **4** exhibits good solubility in THF, but is only moderately soluble in aromatic and aliphatic hydrocarbons. The $^{31}\text{P}\{^1\text{H}\}$ NMR spectrum recorded in C_6D_6 shows a singlet at δ 76.5 ppm with strong ^{199}Hg to ^{31}P coupling ($J_{\text{PHg}} = 333$ Hz). Furthermore, **4** is remarkably stable in C_6D_6 solution, showing no degradation when heated to 80 $^\circ\text{C}$ for 4 days. Crystals suitable for X-ray diffraction were grown by slow evaporation of concentrated benzene solutions at ambient temperatures. \ddagger The solid state structure features a slightly distorted square planar geometry at the nickel atoms with Ni–N distances of 1.922(3) Å and 1.923(3) Å in two independent molecules. To minimize steric hindrance, the two $[(t\text{BuPNP})\text{Ni}]$ fragments are nearly orthogonal to each other (interplanar angles between the five-membered rings are 89.9, corresponding to approximate S_4 symmetry of the first molecule, and 80.5 $^\circ$) and coordinate the Hg atom in a linear fashion. The Ni1–Hg–Ni2 angles are 178.699(13) $^\circ$ and 175.056(13) $^\circ$, and the Ni–Hg distances are 2.6488(4), 2.6491(4), 2.6322(4), 2.6379(4) Å (Fig. 2).

While transition metal complexes with a bridging M–Hg–M fragment are known,¹⁵ the cobalt pincer complex $[(\text{POCOP})\text{Co}]_2(\mu\text{-Hg})$ ($\text{POCOP} = \text{C}_6\text{H}_3\text{-1,3-}[\text{OP}(t\text{Bu})_2]_2$)¹⁶ and the nickel complex

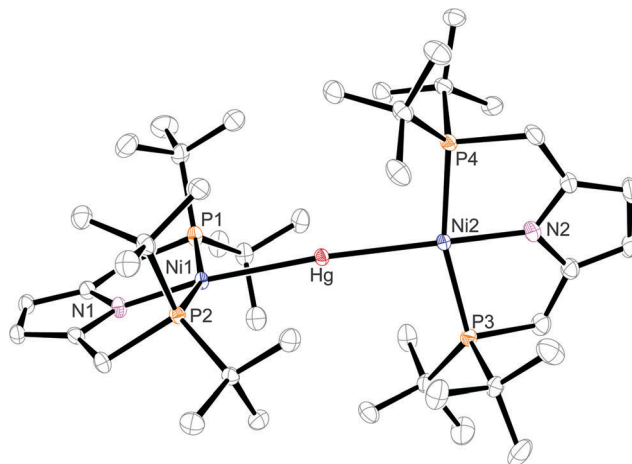


Fig. 2 Displacement ellipsoid plot (50% probability) of one of the two independent molecules of $[(t\text{BuPNP})\text{Ni}]_2(\mu\text{-Hg})$ (**4**). Hydrogen atoms are omitted for clarity. Selected bond distances (Å) and angles ($^\circ$): Ni1–N1 1.922(3), Ni1–P1 2.2191(9), Ni1–P2 2.2230(9), Ni1–Hg 2.6488(4), Ni2–N2 1.921(3), Ni2–P3 2.2248(9), Ni2–P4 2.2174(9), Ni2–Hg 2.6491(4), N1–Ni1–Hg 177.26(8), P1–Ni–P2 162.53(4), N1–Ni1–P1 80.98(8), N1–Ni1–P2 82.44(8), P1–Ni1–Hg 98.24(3), P2–Ni1–Hg 98.58(3), N2–Ni2–Hg 178.95(8), N2–Ni2–P3 82.08(8), N2–Ni2–P4 81.95(8), P3–Ni2–Hg 97.15(3), P4–Ni2–Hg 98.82(3), Ni1–Hg–Ni2 178.699(13). Values for the other molecule are to be found in the deposited material.

$[(\eta^5\text{-C}_5\text{H}_5)\text{Ni}(\text{PET}_3)]_2(\mu\text{-Hg})$ ¹⁷ exhibit similar structural features to **4**. The latter complex was prepared by Hg insertion into the Ni–Ni bond of $[(\eta^5\text{-C}_5\text{H}_5)\text{Ni}(\text{PET}_3)]_2$ and shows a linear Ni–Hg–Ni arrangement with an Ni–Hg distance of 2.468(1) Å,¹⁷ significantly shorter than in **4**. Unfortunately the reactivity of $[(\eta^5\text{-C}_5\text{H}_5)\text{Ni}(\text{PET}_3)]_2(\mu\text{-Hg})$ has not been explored, so the intrinsic reactivity of the $\text{Ni}_2(\mu\text{-Hg})$ fragment is unknown. The cobalt pincer complex $[(\text{POCOP})\text{Co}]_2(\mu\text{-Hg})$ does react with H_2 to yield mixtures of $[(\text{POCOP})\text{Co}(\eta^2\text{-H}_2)]$ and $[(\text{POCOP})\text{CoH}_2(\eta^2\text{-H}_2)]$ depending on the reaction conditions.¹⁶ The question arises whether complex **4** could act as a synthon for two (PNP)Ni(i) fragments and therefore initiate homolytic bond cleavage reactions. A similar reactivity was observed for the well investigated $[(\text{nacnac})\text{Ni}]_2(\mu\text{-N}_2)$ ($\text{nacnac} = \text{HC}(\text{CMeNC}_6\text{H}_3(\text{iPr})_2)_2$), which readily releases N_2 and converts to the corresponding nickel hydride $[(\text{nacnac})\text{Ni}(\mu\text{-H})]_2$.¹⁸

From frontier orbital considerations, taking into account the interactions between the two square-planar Ni(i) PNP fragments (d^9) and $\text{Hg}(0)$, one can readily rationalize the diamagnetism of **4** on the basis of a 3c,2e-bond (Fig. 3). This picture is also supported by more elaborate DFT computations at the B97D level of theory, which show that the computed geometry for the singlet ground state is in good agreement with the experimental data (ESI †). The computed singlet–triplet energy separation (ΔG^0) is 64.3 kJ mol^{-1} ; and thus consistent with the experimentally observed diamagnetic ground state.

To investigate the ability of **4** to act as a suitable synthon for (PNP)Ni(i) fragments, complex **4** was exposed to H_2 . Gratifyingly, when **4** is treated with H_2 (1 atm) metallic Hg precipitates from solution and the nickel(ii) hydride $[(t\text{BuPNP})\text{NiH}]$ (**5b**) can be isolated (Scheme 1 and ESI †). This reaction proceeds slowly at ambient temperature, but complete homolytic cleavage of H_2 can



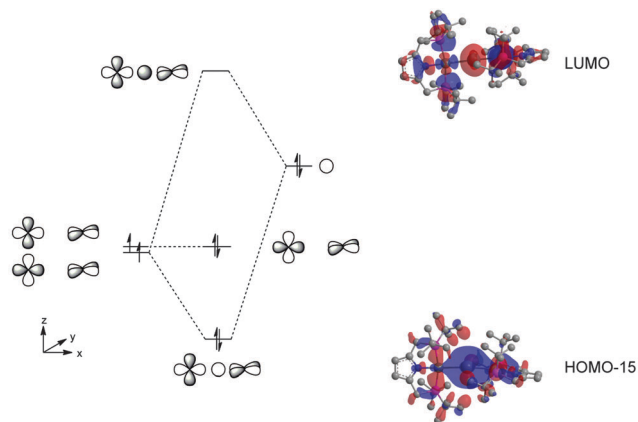


Fig. 3 Frontier orbitals considerations and molecular orbitals (isocontour level at 0.018) of **4** (B97D/6-311G(d,p) (C, H, N, P); SDD (Hg)).

be reached in less than 2 hours when heated to 60 °C. Similar to observations with $[(^{\text{Cy}}\text{PNP})\text{NiH}]$,^{3a} **5b** is thermally stable and no H_2 elimination is observed when heated in C_6D_6 solution. Alternatively, **5b** may also be prepared by oxidative addition of **1b** to $[(\text{cod})_2\text{Ni}]$ (cod = η^4 -cyclooctadiene). However, this method requires thermolysis at 80 °C and 5 bar pressure of H_2 to ensure clean conversion, notably harsher conditions than when the sterically smaller **1a** is employed (ESI†). The monohydride complexes **5a** and **5b** feature a high field-shifted Ni–H resonance in the ^1H NMR spectrum at δ –17.59 and –17.65 ppm, which are split to a triplet with $^2J_{\text{HP}} = 59$ and 56 Hz, respectively. Furthermore a strong absorption in the IR spectrum of **5b** at 1832 cm^{-1} is ascribed to the Ni–H stretch, which is sensitive to isotopic labelling (Ni–D: 1321 cm^{-1} ; ESI†). The solid state structure of **5b** (see ESI† for the X-ray structure of **5a**) shows the expected square planar geometry at the Ni centre and was of sufficient quality that the hydride was successfully located in the difference Fourier map and refined isotropically (Fig. 4). \ddagger The Ni–N and Ni–H distances are 1.8699(9) Å and 1.36(2) Å, respectively, and the N–Ni–H angle is $178.1(7)^\circ$.

Complex **5b** is remarkably stable towards D_2 or C_2H_4 even at elevated temperatures and pressures, displaying neither detectable

isotopic exchange nor insertion (ESI†). The lack of reactivity suggests that ligand coordination *via* the axial site is difficult, which is a consequence of the square-planar d^8 complex geometry and also, to some extent, the steric bulk of the *t*Bu-groups. However, more electrophilic substrates, such as CO_2 , are capable of formally inserting into metal–element bonds without pre-coordination provided that the metal is sufficiently nucleophilic.¹⁹ Indeed, CO_2 insertion into the Ni–H bond is observed for **5a** and **5b** affording the corresponding formate complexes **6a** and **6b** (Scheme 1 and ESI†). The *i*Pr-substituted derivative **6a** forms cleanly at ambient temperature under CO_2 (2.5 bar) and the product was successfully isolated and fully characterised. The solid state structure **6a** features the expected square planar geometry at the nickel atoms with a $\kappa^1\text{O}$ -coordinate formate group (Fig. 5), Ni–O1 1.8914(10) Å. \ddagger The Ni–N distance and N–Ni–O1 angle are 1.8484(11) Å and $175.22(5)^\circ$, respectively. The long through-space distance Ni...O2, 2.937(1) Å indicates that the formate group is a monodentate ligand and also supports the idea that the binding of a fifth ligand is difficult for electronic reasons.

However, heating of **6a** in C_6D_6 at 100 °C in a sealed tube shows that CO_2 is released and **5a** is reformed, whereas on standing at ambient temperature CO_2 reinserts into the Ni–H bond to form the thermodynamically preferred **6a**. In contrast, CO_2 insertion into **5b** required heating of the reaction mixture at 80 °C under 5 bar pressure of CO_2 for 2 h to achieve partial conversion to formate **6b**. The latter observation underlines the steric influence of the phosphine substituents on the CO_2 insertion chemistry.

The pyrrolyl-based PNP ligands **1** can readily be prepared and used for the synthesis of (PNP)Ni complexes. Reduction of $[(^{\text{tBu}}\text{PNP})\text{NiBr}]$ with Na/Hg gives the unique $[(^{\text{tBu}}\text{PNP})\text{Ni}]_2(\mu\text{-Hg})$ (**4**), which is diamagnetic because of a 3c,2e-bond formed within the Ni_2Hg moiety. Upon addition of a suitable substrate, complex **4** can act as a synthon for two $(^{\text{tBu}}\text{PNP})\text{Ni}(\text{I})$ fragments, as illustrated by the homolytic cleavage of H_2 to furnish $[(^{\text{tBu}}\text{PNP})\text{NiH}]$ (**5b**). Further investigations with these PNP ligands to stabilize low-valent 3d-metals are ongoing and will be reported in due course.

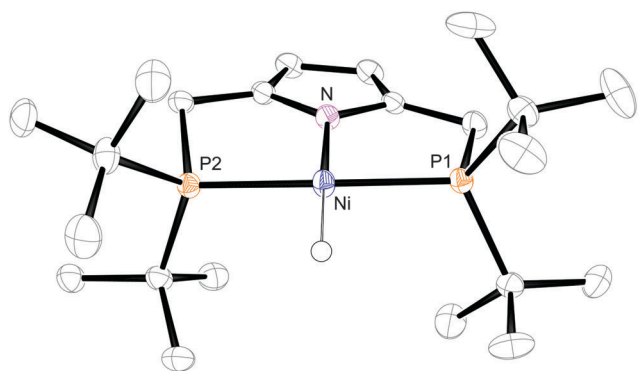


Fig. 4 Displacement ellipsoid plot (50% probability) of $[(^{\text{tBu}}\text{PNP})\text{NiH}]$ (**5b**). Hydrogen atoms, except Ni–H, are omitted for clarity. Selected bond distances (Å) and angles ($^\circ$): Ni–N 1.8699(9), Ni–P1 2.1587(3), Ni–P2 2.1611(3), Ni–H 1.36(2), N–Ni–H $178.1(7)$, P1–Ni–P2 $169.378(11)$, N–Ni–P1 $85.71(3)$, N–Ni–P2 $85.30(3)$, P1–Ni–H $92.6(7)$, P2–Ni–H $96.3(7)$.

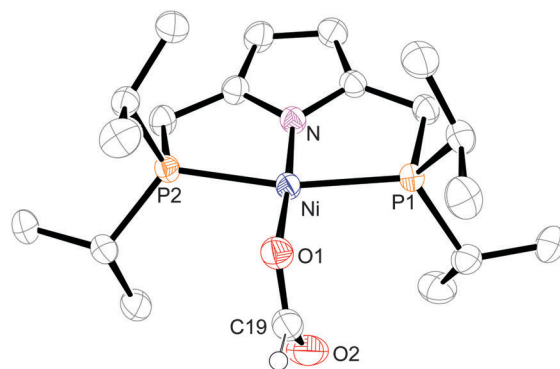


Fig. 5 Displacement ellipsoid plot (50% probability) of $[(^{\text{iPr}}\text{PNP})\text{NiOC(O)H}]$ (**6a**). Hydrogen atoms, except the H-atom attached to C19, are omitted for clarity. Selected bond distances (Å) and angles ($^\circ$): Ni–N 1.8484(11), Ni–O1 1.8914(10), Ni–P1 2.2123(4), Ni–P2 2.1954(4), O1–C19 1.2754(19), C19–O2 1.216(2), N–Ni–O1 $175.22(5)$, P1–Ni–P2 $167.392(17)$, N–Ni–P1 $84.69(4)$, N–Ni–P2 $84.40(4)$. Through-space Ni...O2 distance: 2.937(1) Å.



We acknowledge the financial support by the Deutsche Forschungsgemeinschaft (DFG) through the Emmy Noether program (WA 2513/2) (MDW) and by the National Science Foundation (CHE-1350047) (WHB).

Notes and references

‡ Crystal structure data for **3b**: $C_{22}H_{42}BrNNiP_2$, $M = 521.13$, orthorhombic, $a = 11.4257(2)$ Å, $b = 14.4710(3)$ Å, $c = 15.0601(3)$ Å, $V = 2490.06(8)$ Å³, $T = 100(2)$ K, space group $P2_12_12_1$, $Z = 4$, $\mu(\text{Cu K}\alpha) = 4.3$ mm⁻¹, 52 074 reflections measured, 5154 independent ($R_{\text{int}} = 0.054$). R values: $wR(F^2)$ 0.0599 (all data), R_1 0.0241 ($I > 2\sigma(I)$); $S(F^2)$ 1.03, Flack parameter $-0.011(14)$. Crystal structure data for **4** (C_6H_6): $C_{50}H_{90}HgN_2Ni_2P_4$, $M = 1161.13$, triclinic, $a = 13.9339(5)$ Å, $b = 16.4179(5)$ Å, $c = 24.9947(8)$ Å, $\alpha = 108.376(3)^\circ$, $\beta = 96.539(3)^\circ$, $\gamma = 97.870(3)^\circ$, $V = 5299.7(3)$ Å³, $T = 100(2)$ K, space group $P1$, $Z = 4$, $\mu(\text{Mo K}\alpha) = 3.7$ mm⁻¹, 294 221 reflections measured, 31 636 independent ($R_{\text{int}} = 0.092$). R values: $wR(F^2)$ 0.0760 (all data), R_1 0.0403 ($I > 2\sigma(I)$); $S(F^2)$ 1.03. Crystal structure data for **5b**: $C_{22}H_{43}NNiP_2$, $M = 442.22$, orthorhombic, $a = 11.0422(2)$ Å, $b = 14.7303(2)$ Å, $c = 14.7768(2)$ Å, $V = 2403.53(6)$ Å³, $T = 100(2)$ K, space group $P2_12_12_1$, $Z = 4$, $\mu(\text{Mo K}\alpha) = 0.94$ mm⁻¹, 209 772 reflections measured, 7458 independent ($R_{\text{int}} = 0.048$). R values: $wR(F^2)$ 0.0474 (all data), R_1 0.0204 ($I > 2\sigma(I)$); $S(F^2)$ 1.06, Flack parameter $-0.010(6)$. Crystal structure data for **6a**: $C_{19}H_{35}NNiO_2P_2$, $M = 430.13$, orthorhombic, $a = 15.7937(4)$ Å, $b = 13.5622(3)$ Å, $c = 20.6530(5)$ Å, $V = 4423.79(18)$ Å³, $T = 130(2)$ K, space group $Pbca$, $Z = 8$, $\mu(\text{Cu K}\alpha) = 2.7$ mm⁻¹, 42 437 reflections measured, 4648 independent reflections ($R_{\text{int}} = 0.044$). R values: $wR(F^2)$ 0.0667 (all data), R_1 0.0257 ($I > 2\sigma(I)$); $S(F^2)$ 1.04.

- (a) M. E. van der Boom and D. Milstein, *Chem. Rev.*, 2003, **103**, 1759–1792; (b) *The Chemistry of Pincer Compounds*, ed. D. Morales-Morales and C. Jensen, Elsevier, Amsterdam, 2007; (c) C. Gunanathan and D. Milstein, *Acc. Chem. Res.*, 2011, **44**, 588–602; (d) D. Gelman and R. Romm, *Top. Organomet. Chem.*, 2013, **40**, 289–317; (e) D. Roddick, *Top. Organomet. Chem.*, 2013, **40**, 49–88; (f) G. van Koten, *Top. Organomet. Chem.*, 2013, **40**, 1–20; (g) *Pincer and Pincer-Type Complexes: Applications in Organic Synthesis and Catalysis*, ed. K. J. Szabó and O. F. Wendt, Wiley-VCH, Weinheim, 2014.
- (a) L. Zhang, Z. Zuo, X. Wan and Z. Huang, *J. Am. Chem. Soc.*, 2014, **136**, 15501–15504; (b) L. Zhang, Z. Zuo, X. Leng and Z. Huang, *Angew. Chem., Int. Ed.*, 2014, **53**, 2696–2700; (c) D. Peng, Y. Zhang, X. Du, L. Zhang, X. Leng, M. D. Walter and Z. Huang, *J. Am. Chem. Soc.*, 2013, **135**, 19154–19166.
- (a) G. T. Venkanna, S. Tammineni, H. D. Arman and Z. J. Tonzetich, *Organometallics*, 2013, **32**, 4656–4663; (b) G. T. Venkanna, H. D. Arman and Z. J. Tonzetich, *ACS Catal.*, 2014, **4**, 2941–2950.
- J. V. Obligation, S. P. Semproni and P. J. Chirik, *J. Am. Chem. Soc.*, 2014, **136**, 4133–4136.
- (a) S. Chakraborty, J. Zhang, J. A. Krause and H. Guan, *J. Am. Chem. Soc.*, 2010, **132**, 8872–8873; (b) S. Chakraborty, J. Zhang, Y. J. Patel, J. A. Krause and H. Guan, *Inorg. Chem.*, 2013, **52**, 37–47.

- (a) E. A. Bielinski, P. O. Lagaditis, Y. Zhang, B. Q. Mercado, C. Wurtele, W. H. Bernskoetter, N. Hazari and S. Schneider, *J. Am. Chem. Soc.*, 2014, **136**, 10234–10237; (b) S. Chakraborty, P. O. Lagaditis, M. Forster, E. A. Bielinski, N. Hazari, M. C. Holthausen, W. D. Jones and S. Schneider, *ACS Catal.*, 2014, **4**, 3994–4003.
- (a) Z.-X. Wang and N. Liu, *Eur. J. Inorg. Chem.*, 2012, 901–911; (b) D. Gallego, A. Brueck, E. Irran, F. Meier, M. Kaupp, M. Driess and J. F. Hartwig, *J. Am. Chem. Soc.*, 2013, **135**, 15617–15626.
- K. V. Vasudevan, B. L. Scott and S. K. Hanson, *Eur. J. Inorg. Chem.*, 2012, 4898–4906.
- G. T. Venkanna, T. V. M. Ramos, H. D. Arman and Z. J. Tonzetich, *Inorg. Chem.*, 2012, **51**, 12789–12795.
- N. Grüger, H. Wadehoff and L. H. Gade, *Dalton Trans.*, 2012, **41**, 14028–14030.
- S. Kumar, G. Mani, S. Mondal and P. K. Chattaraj, *Inorg. Chem.*, 2012, **51**, 12527–12539.
- (a) M. D. Fryzuk, A. Carter and A. Westerhaus, *Inorg. Chem.*, 1985, **24**, 642–648; (b) M. D. Fryzuk, D. B. Leznoff, E. S. F. Ma, S. J. Rettig and V. G. Young, Jr., *Organometallics*, 1998, **17**, 2313–2323; (c) M. D. Fryzuk, D. B. Leznoff, R. C. Thompson and S. J. Rettig, *J. Am. Chem. Soc.*, 1998, **120**, 10126–10135; (d) H. Fan, B. C. Fullmer, M. Pink and K. G. Caulton, *Angew. Chem., Int. Ed.*, 2008, **47**, 9112–9114; (e) B. C. Fullmer, H.-J. Fan, M. Pink, J. C. Huffman, N. P. Tsvetkov and K. G. Caulton, *J. Am. Chem. Soc.*, 2011, **133**, 2571–2582.
- (a) O. V. Ozerov, C. Guo, V. A. Papkov and B. M. Foxman, *J. Am. Chem. Soc.*, 2004, **126**, 4792–4793; (b) B. C. Bailey, H. Fan, J. C. Huffman, M.-H. Baik and D. J. Mindiola, *J. Am. Chem. Soc.*, 2006, **128**, 6798–6799; (c) L.-C. Liang, P.-S. Chien, J.-M. Lin, M.-H. Huang, Y.-L. Huang and J.-H. Liao, *Organometallics*, 2006, **25**, 1399–1411; (d) M. T. Whited and R. H. Grubbs, *J. Am. Chem. Soc.*, 2008, **130**, 16476–16477; (e) J. G. Andino, U. J. Kilgore, M. Pink, A. Ozarowski, J. Krzystek, J. Telser, M.-H. Baik and D. J. Mindiola, *Chem. Sci.*, 2010, **1**, 351–356.
- J. A. Kessler and V. M. Iluc, *Inorg. Chem.*, 2014, **53**, 12360–12371.
- (a) J. Bauer, H. Braunschweig and R. D. Dewhurst, *Chem. Rev.*, 2012, **112**, 4329–4346; (b) D. C. Rosenfeld, P. T. Wolczanski, K. A. Barakat, C. Buda and T. R. Cundari, *J. Am. Chem. Soc.*, 2005, **127**, 8262–8263.
- T. J. Hebdon, A. J. S. John, D. G. Gusev, W. Kaminsky, K. I. Goldberg and D. M. Heinekey, *Angew. Chem., Int. Ed.*, 2011, **50**, 1873–1876.
- J. J. Schneider, U. Denninger, J. Hagen, C. Krüger, D. Bläser and R. Boese, *Chem. Ber.*, 1997, **130**, 1433–1440.
- S. Pfirrmann, S. Yao, B. Ziemer, R. Stösser, M. Driess and C. Limberg, *Organometallics*, 2009, **28**, 6855–6860.
- (a) T. Fan, X. Chen and Z. Lin, *Chem. Commun.*, 2012, **48**, 10808–10828; (b) H.-W. Suh, T. J. Schmeier, N. Hazari, R. A. Kemp and M. K. Takase, *Organometallics*, 2012, **31**, 8225–8236; (c) J. Li and K. Yoshizawa, *Bull. Chem. Soc. Jpn.*, 2011, **84**, 1039–1048; (d) A. Urakawa, F. Jutz, G. Laurenczy and A. Baiker, *Chem. – Eur. J.*, 2007, **13**, 3886–3899; (e) T. Matsubara and K. Hirao, *Organometallics*, 2001, **20**, 5759–5768; (f) B. P. Sullivan and T. J. Meyer, *Organometallics*, 1986, **5**, 1500–1502.

